Published in final edited form as:
J Magn Reson Imaging. 2011 June ; 33(6): 1382–1389. doi:10.1002/jmri.22567.

The diverse pathology and kinetics of mass, nonmass and focus enhancement on MR imaging of the breast

Sanaz A. Jansen, PhD[1,¶], **Akiko Shimauchi, MD**[1], **Lindsay Zak, BSc**[1], **Xiaobing Fan, PhD**[1], **Gregory S. Karczmar, PhD**[1], and **Gillian M. Newstead, MD**[1,*]

[1] Department of Radiology, The University of Chicago, 5841 S. Maryland Ave MC2026, Chicago, IL 60637

Abstract

Purpose—To compare the pathology and kinetic characteristics of breast lesions with focus, mass and nonmass-like enhancement.

Materials and Methods—852 MRI detected breast lesions in 697 patients were selected for an IRB approved review. Patients underwent dynamic contrast enhanced MRI using one pre and three to six post-contrast T_1 weighted images. The 'type' of enhancement was classified as mass, non-mass or focus, and kinetic curves quantified by the initial enhancement percentage (**E_1**), time to peak enhancement (**T_{peak}**) and signal enhancement ratio (**SER**). These kinetic parameters were compared between malignant and benign lesions within each morphologic type.

Results—552 lesions were classified as mass (396 malignant, 156 benign), **261** as nonmass (212 malignant,49 benign) and **39** as focus (9 malignant,30 benign). The most common pathology of malignant/benign lesions by morphology: for mass, invasive ductal carcinoma/fibroadenoma; for nonmass, ductal carcinoma in situ (DCIS)/fibrocystic change(FCC); for focus, DCIS/FCC. Benign mass lesions exhibited significantly lower **E_1**, longer **T_{peak}** and lower **SER** compared with malignant mass lesions ($p < 0.0001$). Benign nonmass lesions exhibited only a lower **SER** compared to malignant nonmass lesions ($p<0.01$).

Conclusions—By considering the diverse pathology and kinetic characteristics of different lesion morphologies, diagnostic accuracy may be improved.

Keywords

breast DCE-MRI; nonmass-like enhancement; contrast media kinetics; morphology; diagnostic accuracy; malignant

INTRODUCTION

The high sensitivity of dynamic contrast enhanced magnetic resonance imaging (DCE-MRI) for the detection of invasive breast cancer has expanded its clinical role to include high risk screening, pre-operative staging, and post-treatment follow-up (1,2). Several prior reports have shown that DCE-MRI provides excellent depiction of lesion morphology and, compared to other imaging modalities, most accurately determines pathologic disease extent (3–5). In addition, qualitative and quantitative measures of contrast media uptake and washout—or kinetic—time course curves provides a functional lesion characterization, and

[*]Corresponding Author: Professor Gillian Newstead, M.D., Department of Radiology, University of Chicago, 5841 S. Maryland Ave, MC 2026, Chicago, IL 60637, Phone: (773) 702-2781, Fax: (773) 834-9047, gnewstead@radiology.bsd.uchicago.edu.
[¶]Currently at Mouse Cancer Genetics Program, National Cancer Institute, Frederick Maryland

have been correlated with biomarkers, such as microvessel density, proliferative index and nuclear grade (6,7). Thus, DCE-MRI of the breast allows for simultaneous characterization of lesion morphology and physiology, the latter via analysis of kinetic curves.

Classification of morphology according to the Breast Imaging Reporting and Data System (BIRADS) lexicon (8) begins with categorizing the 'type' of enhancement as focus, mass or nonmass-like (Figure 1). According to the same lexicon, kinetic curves are classified as exhibiting a 'washout', 'plateau' or 'persistent' shape(9). Mass lesions are the most common finding: benign mass lesions are often round or oval in shape, with smooth margins, and exhibit 'persistent' type curves, while malignant mass lesions are often irregularly shaped, with irregular or spiculated margins and display 'washout' type curves (10,11). Nonmass-like enhancement is less common although it is the predominant morphology of preinvasive ductal carcinoma *in situ* (DCIS) which exhibits a variety of kinetic curve shapes (12–14). While several reports have documented the morphologic and kinetic characteristics of benign and malignant lesions, few have studied the relationship between lesion morphology and kinetics in a large number of patients (15–17). Such analysis is desirable, as differential diagnosis will most often involve distinguishing benign from malignant lesions of the same morphologic type—it is unlikely a malignant nonmass lesion would be mistaken for a benign mass lesion, and vice versa.

Indeed, it is likely that focus, mass and nonmass enhancement patterns reflect fundamental differences in underlying lesion pathology, physiology and biology, which may in turn affect their kinetic curve characteristics. Consequently, the kinetic parameters and criteria that work best to distinguish benign and malignant mass lesions may not work as well with focus or non-mass lesions. In this study we set out to categorize the pathology and kinetic characteristics of focus, mass and nonmass-like enhancement in a large patient population, including performing qualitative and quantitative kinetic analysis and measures of diagnostic accuracy in each type of enhancement.

MATERIALS AND METHODS

Patients

At our institution, we maintain a HIPAA compliant research database in which patient image data for this study was collected under an IRB approved waiver of consent. For each patient presenting for DCE-MRI of the breast, the database stores the radiologist-determined MRI findings. In addition, the corresponding pathologic diagnosis for each MR detected lesion is recorded (when available) based on consensus opinion of two pathologists. The most common indications for breast DCE-MRI are pre-operative staging of newly diagnosed cancers, postoperative and treatment follow-up, and screening of women at high-risk for developing breast cancer. A retrospective review of 697 consecutive patients with pathologic findings yielded 852 lesions that were histologically proven to be either benign lesions or newly-diagnosed cancers. The average patient age was 54.5 ±13.6 years, and average lesion size was 21.5±18.9 mm. After review of final pathology reports, 235 lesions were determined to be benign and 617 malignant. The malignant lesions were further classified as invasive ductal carcinoma (IDC), ductal carcinoma *in situ* (DCIS), invasive lobular carcinoma (ILC) or 'other' based on review of final pathology reports. Similarly, the benign lesions were classified as fibroadenoma, papilloma, fibrocystic change (FCC), breast tissue, or 'other'.

MR Imaging Protocol and Analysis

MR imaging was performed using three different imaging systems, as detailed in Table 1. Patients were all imaged in the prone position, and obtained pre-contrast T_2-weighted fast

spin echo acquisitions in the axial plane. For DCE-MRI scans, a 3D T1 weighted imaging protocol was utilized with primary acquisition in either the coronal or axial plane. 20 ml of 0.5mmol/ml Gadodiamide (Omniscan; Nycomed-Amersham, Princeton, NJ) was injected intravenously followed by a 20 ml saline flush at the rate of 2.0 ml/sec. Twenty seconds after contrast administration the first post-contrast acquisition was started, and for all examinations the first, second and last post-contrast dataset were acquired after approximately one, two and six minutes, respectively. All analysis of lesion enhancement (morphology and kinetics) was performed on subtraction images.

As part of routine clinical reporting at our institution, the morphology of each MR detected lesion is prospectively analyzed according to the BIRADS lexicon, beginning with classification of the type of enhancement as ‘mass’, ‘nonmass’ or ‘focus’ (9). This morphology assessment is performed under consensus opinion of two radiologists, and is blinded to the lesion final pathology (although not necessarily prior biopsy findings).

Previously observed significant differences between kinetic curves acquired on different MR systems precluded pooling of kinetic data (18). Thus, only lesions imaged on System A were used for qualitative and quantitative analysis of lesion contrast kinetics, due to the substantially larger number and the more representative distribution of mass, nonmass and focus lesions included (Table 1). A total of 574 lesions were thus included for kinetic analysis, of which 403 were malignant and 171 benign. One experienced radiologist retrospectively reviewed the images at least one year after the morphology classification, and was blinded to the lesion pathology and final MRI interpretation. To generate the kinetic curve, the radiologist used institutional software written in IDL (Research Systems, Inc., Boulder, CO, USA) to allow for manual generation of kinetic curves and subsequent extraction of kinetic curve data points to facilitate further mathematical analysis. The radiologist traced a small region of interest (ROI) around what was perceived to be the most enhancing part of the lesion on the first post-contrast image. The plot of signal intensity vs. time for this ROI was assessed by the radiologist according to the BIRADS lexicon, which describes the initial rise (‘rapid’, ‘medium’, ‘slow’) and delayed phase (‘persistent’, ‘plateau’, ‘washout’) of the kinetic curve(9). In addition to this qualitative assessment of kinetics, several quantitative parameters were calculated: the initial and peak enhancement percentages ($\mathbf{E_1}$ and $\mathbf{E_{peak}}$), the time to peak enhancement ($\mathbf{T_{peak}}$) in seconds (10), and the signal enhancement ratio (**SER**) a measure of contrast media washout relative to the first post contrast point (19).

Statistical Analysis

The distribution of pathology subtypes were compared between mass and nonmass lesions using the Pearson’s χ^2 – test. Similarly, to compare the proportion of ‘washout’ vs. ‘plateau’ and ‘persistent’ curves (or ‘rapid’ vs. ‘medium’ and ‘slow’) the Pearson’s χ^2 – test was used. For large sample (n >30) comparisons, the two-tailed unequal variance Student’s *t*-test was performed to evaluate which quantitative kinetic parameters showed significant differences between focus, mass and nonmass lesions, as well as in subpopulations of benign and malignant. For small sample comparisons (n <30), the Mann-Whitney rank and rum test was used. For all statistical analysis, a *p* value less than 0.05 was considered statistically significant. The Holm-Bonferroni correction method was used to account for multiple comparisons(20).

The sensitivity and specificity of BIRADS kinetic descriptors were calculated separately in focus, mass and nonmass lesions. In addition, receiver operating characteristic (ROC) analysis was performed to compare the diagnostic performance of the kinetic parameters in the whole population, as well as in subpopulations of focus, mass and nonmass lesions.

ROCKIT software (ROCKIT 0.9B Beta Version) was used to generate the ROC curves and to compare area under the curve (A_z) values using the area test.

RESULTS

Pathology of Focus, Mass and Nonmass Lesions

Overall, **552** lesions were classified as exhibiting mass-like enhancement, with 71.7% (396/552) malignant and 28.3% (156/552) benign; **261** were classified as nonmass lesions, with 81.2% (212/261) malignant and 18.8% (49/261) benign; **39** were classified as focus, with 23.1% (9/39) malignant and 76.9% (30/39) benign. Malignant mass and nonmass lesions differed significantly in their pathology subtype breakdown ($p < 0.0001$ by χ^2-test) where the former were predominantly IDC and the latter predominantly DCIS (Table 2). Similarly, benign mass and nonmass lesions exhibited significantly different pathologies ($p < 0.002$), with fibroadenomas comprising the largest proportion of benign mass lesions and FCC the largest proportion of benign nonmass lesions (Table 2). The predominant pathology of focus lesions was FCC and breast tissue. The average lesion size of malignant mass lesions was 20.6±14.9 mm, while benign mass lesions were smaller, at 10.3±4.2 mm on average. Malignant nonmass lesions extended 36.1±24.8 mm on average, compared to benign nonmass lesions at 18.9±12.2 mm.

Kinetics of Focus, Mass and Nonmass Lesions

Kinetic curves (Figure 2) were generated in 574 lesions, of which 360 were classified as exhibiting mass-like enhancement, with 69.7% (251/360) malignant and 30.3% (109/360) benign; 182 were classified as nonmass lesions, with 79.7% (145/182) malignant and 20.3% (37/182) benign; 32 were classified as focus, with 21.9% (7/32) malignant and 78.1% (25/32) benign. Overall, mass lesions (benign or malignant) exhibited a higher proportion of curves classified as ‘rapid’ initial uptake and ‘washout’ delayed phase compared with nonmass and focus lesions (p <0.02, Figure 3). Malignant mass lesions demonstrated a significantly higher proportion of curves classified as having ‘rapid’ initial rise at 91%, compared to benign mass lesions at 59% ($p < 0.001$). In addition, 72% of malignant mass lesions exhibited ‘washout’ type curves, compared to only 34% of benign mass lesions ($p < 0.0001$). Analysis in nonmass lesions yielded similar findings: malignant vs. benign nonmass lesions displayed an increased proportion of curves classified as ‘rapid’ initial rise (77% vs. 54%, p<0.03) and ‘washout’ delayed phase (54% vs. 17%, p< 0.0002).

Quantitative kinetic analysis revealed similar trends. Mass lesions, regardless of pathology, exhibited statistically significant differences compared with nonmass lesions (Table 3), including higher $\mathbf{E_1}$ (285% vs. 210%, $p<10^{-7}$), $\mathbf{E_{peak}}$ (348% vs. 265%, $p<10^{-7}$), **SER** (1.02 vs. 0.90, $p < 0.0009$) and shorter $\mathbf{T_{peak}}$ (167 sec vs. 209 sec, $p < 0.0001$). Malignant mass lesions exhibited considerably larger $\mathbf{E_1}$, **SER** and shorter $\mathbf{T_{peak}}$ compared with benign mass lesions (Table 3, $p < 10^{-6}$), whereas nonmass malignant lesions exhibited only significantly higher **SER** i.e., stronger washout, compared with nonmass benign lesions (0.93 vs. 0.76, p=0.008). For focus lesions, no statistically significant differences were found between benign and malignant subtypes ($p > 0.4$ by Mann-Whitney test).

For the qualitative descriptors of contrast media kinetics, sensitivity increased while specificity decreased slightly in mass lesions, although 95% confidence intervals for specificity values demonstrated considerable overlap among types of enhancement. To evaluate diagnostic performance of the quantitative kinetic parameters, ROC analysis yielded A_z values for each kinetic parameter evaluated in the whole population, as well as separately in focus, mass and nonmass lesions (Table 4). A_z values were higher in mass compared to nonmass and focus lesions for all parameters except $\mathbf{E_{peak}}$, although these

differences were not statistically significant ($p > 0.06$). The parameter **SER** provided the highest diagnostic accuracy for both mass and nonmass lesions. ROC curves of **SER** in focus, mass and nonmass lesions are displayed in Figure 4 and show that at a sensitivity of ~ 80% the specificity of **SER** is 55% in mass lesions, and only 35% and 25% in nonmass and focus lesions, respectively.

DISCUSSION

Over a decade of studies have culminated in the conventional kinetic standards used today to distinguish benign from malignant breast lesions(11,21–22). However, improvements in diagnostic accuracy of kinetic analysis are still needed, as many benign and malignant lesions exhibit considerable kinetic overlap. If a radiologist is presented with a mass, nonmass or focus lesion of unknown pathology, is the diagnostic accuracy of conventional kinetic analysis equally effective in these different types of lesions? To address this question, we have performed to our knowledge the largest single institution study relating quantitative kinetic and pathologic characteristics to lesion morphology (15–17,22–31). Our results suggest that quantitative kinetic parameters are more diagnostically useful in mass lesions compared to nonmass lesions, and not effective for focus enhancement. With high significance, malignant mass lesions exhibited faster contrast uptake, shorter time to peak enhancement, and stronger washout compared to benign mass lesions. In comparison, nonmass malignant and benign lesions differed significantly only in the washout parameter **SER**.

Interestingly, for both mass and nonmass lesions **SER** proved to be the most diagnostically useful kinetic parameter, underscoring its previously demonstrated robustness and utility (19,32–33). This is in contrast to prior reports analyzing contrast kinetics in smaller populations of nonmass lesions (15–16), wherein the diagnostic accuracy of kinetic parameters of both uptake and washout was poor. Thus, our results do suggest a path forward to improving diagnostic accuracy in nonmass lesions via enhanced analysis of lesion washout, for example, by using an automated algorithm to select a representative kinetic curve (34), or by applying measures of kinetic heterogeneity (16,35). In addition, acquiring DCE-MRI data at higher temporal resolution may also improve diagnostic accuracy by providing a refined quantitative measure of contrast kinetics (36–38). Employing novel imaging techniques including spectroscopic (23) and diffusion-weighted (27) imaging may also aid in lesion characterization, as would analysis of other morphologic descriptors, such as distribution or internal enhancement pattern (17,25,39).

Exploring these and other strategies to improve the reliable identification of malignant nonmass and focus lesions by DCE-MRI is an important clinical goal. Prior reports have noted that the increased false-positive rates of DCE-MRI for these types of lesions is a drawback limiting its widespread use (17,40–41). Others have pointed out that the considerable overlap of kinetic patterns of DCIS with benign lesions compromises its reliable identification (13,39,42–43). Focus lesions are particularly challenging; the malignant foci in our study exhibited conventionally benign kinetic characteristics, although generalization is not possible due to the small number of focus lesions included. For this type of enhancement the path to increased diagnostic accuracy is not clear, as foci are by definition too small to be characterized morphologically or to exhibit kinetic heterogeneity.

Our results demonstrate that mass, nonmass and focus-type enhancement patterns reflect not only different morphologic categories but also distinct pathologies and kinetic patterns. Overall, mass lesions, regardless of whether benign or malignant, showed significantly higher contrast uptake than nonmass and focus lesions, as well as earlier time to peak enhancement and stronger washout. These stark morphologic and kinetic differences are

likely related to fundamental differences in underlying lesion physiology; understanding the physiologic basis for contrast media kinetics may aid in the development of improved mathematical modeling and interpretation of kinetic data that can ultimately improve sensitivity and specificity of kinetic analysis. For example, it was recently suggested that contrast uptake of DCIS—which comprised half the nonmass lesions in our study — may be due to gadolinium penetrating through leaky basement membranes of neoplastic ducts and collecting in the lumen(44). This observation could help to explain the nonmass-like enhancement pattern of DCIS, the persistent and plateau curve type often noted for these lesions, and could improve modeling of contrast kinetics in nonmass lesions.

There are several limitations to this study. First, only those benign lesions that were suspicious enough to warrant biopsy and pathologic evaluation were included. This will result in a biased kinetic and pathologic distribution, since most obviously benign lesions would not be sent for pathologic evaluation. Second, the kinetic curves of nonmass lesions and enhancing foci are vulnerable to partial volume effects, as small ROI's placed on the lesion may also capture portions of the surrounding normal tissue. Third, the imaging protocols used varied in dose and temporal sampling, which may affect the reliability of some kinetic parameters. Importantly, prior studies have demonstrated that the parameter **SER** is not adversely affected by these inconsistencies(45), and thus our findings regarding the diagnostic utility of **SER** are not compromised. Finally, kinetic analysis was performed only on one curve selected manually by one radiologist. While our study does not address variability in kinetic measurements between readers, one of the strengths is the large number of mass and particularly nonmass lesions included (22–23,28–31), so that variability in kinetic characteristics between lesions can be accounted for.

To summarize, by analyzing 852 breast lesions on MRI we have found that mass, non-mass and focus type enhancement reflect not only fundamentally different morphologies but also diverse pathologies and kinetic characteristics. This observation may be useful for computer-aided diagnosis systems, suggesting that diagnostic accuracy can be improved if kinetic classifiers are trained separately in lesions based on type of enhancement, or if multiple-class classifiers are used (46). Our results also indicate that the efficacy of kinetic analysis is improved in mass lesions compared to nonmass and focus lesions, and accordingly that kinetic analysis should be performed after morphology assessment: in mass lesions, parameters related to both uptake and washout are of diagnostic utility, while in nonmass lesions only washout parameters may be relevant. Although the significance of our results should be strengthened and established in larger groups of patients with different imaging platforms, this work suggests that tailoring appropriate kinetic feature selection to lesion morphology may help optimize the diagnostic accuracy of DCE-MRI.

Acknowledgments

GRANT SUPPORT: We would like to thank the Segal Foundation, NIH grant P50 CA125183-01 (SPORE) and the Department of Defense Predoctoral Award WX81XWH-06-1-0329 for financial support.

References

1. Newstead GM. MR imaging in the management of patients with breast cancer. Semin Ultrasound CT MR. 2006; 27:320–332. [PubMed: 16916000]
2. Saslow D, Boetes C, Burke W, et al. American Cancer Society guidelines for breast screening with MRI as an adjunct to mammography. CA Cancer J Clin. 2007; 57:75–89. [PubMed: 17392385]
3. Beatty JD, Porter BA. Contrast-enhanced breast magnetic resonance imaging: the surgical perspective. Am J Surg. 2007; 193:600–605. discussion 605. [PubMed: 17434364]
4. Esserman LJ, Kumar AS, Herrera AF, et al. Magnetic resonance imaging captures the biology of ductal carcinoma in situ. J Clin Oncol. 2006; 24:4603–4610. [PubMed: 17008702]

5. Kuhl C, Kuhn W, Braun M, Schild H. Pre-operative staging of breast cancer with breast MRI: one step forward, two steps back? Breast. 2007; 16 (Suppl 2):S34–44. [PubMed: 17959382]
6. Teifke A, Behr O, Schmidt M, et al. Dynamic MR imaging of breast lesions: correlation with microvessel distribution pattern and histologic characteristics of prognosis. Radiology. 2006; 239:351–360. [PubMed: 16569783]
7. Szabo BK, Aspelin P, Kristoffersen Wiberg M, Tot T, Bone B. Invasive breast cancer: correlation of dynamic MR features with prognostic factors. Eur Radiol. 2003; 13:2425–2435. [PubMed: 12898176]
8. Molleran V, Mahoney MC. The BI-RADS breast magnetic resonance imaging lexicon. Magn Reson Imaging Clin N Am. 2010; 18:171–185. vii. [PubMed: 20494304]
9. ACR. American College of Radiology (ACR) Breast Imaging Reporting and Data System Atlas (BI-RADS). Reston, VA: 2003.
10. Szabo BK, Aspelin P, Wiberg MK, Bone B. Dynamic MR imaging of the breast. Analysis of kinetic and morphologic diagnostic criteria. Acta Radiol. 2003; 44:379–386. [PubMed: 12846687]
11. Kuhl CK, Mielcareck P, Klaschik S, et al. Dynamic breast MR imaging: are signal intensity time course data useful for differential diagnosis of enhancing lesions? Radiology. 1999; 211:101–110. [PubMed: 10189459]
12. Groves AM, Warren RM, Godward S, Rajan PS. Characterization of pure high-grade DCIS on magnetic resonance imaging using the evolving breast MR lexicon terminology: can it be differentiated from pure invasive disease? Magn Reson Imaging. 2005; 23:733–738. [PubMed: 16198828]
13. Jansen SA, Newstead GM, Abe H, Shimauchi A, Schmidt RA, Karczmar GS. Pure ductal carcinoma in situ: kinetic and morphologic MR characteristics compared with mammographic appearance and nuclear grade. Radiology. 2007; 245:684–691. [PubMed: 18024450]
14. Viehweg P, Lampe D, Buchmann J, Heywang-Kobrunner SH. In situ and minimally invasive breast cancer: morphologic and kinetic features on contrast-enhanced MR imaging. Magma. 2000; 11:129–137. [PubMed: 11154954]
15. Jansen SA, Fan X, Karczmar GS, et al. DCEMRI of breast lesions: is kinetic analysis equally effective for both mass and nonmass-like enhancement? Med Phys. 2008; 35:3102–3109. [PubMed: 18697535]
16. Newell D, Nie K, Chen JH, et al. Selection of diagnostic features on breast MRI to differentiate between malignant and benign lesions using computer-aided diagnosis: differences in lesions presenting as mass and non-mass-like enhancement. Eur Radiol. 2009; 20:771–781. [PubMed: 19789878]
17. Baltzer PA, Benndorf M, Dietzel M, Gajda M, Runnebaum IB, Kaiser WA. False-positive findings at contrast-enhanced breast MRI: a BI-RADS descriptor study. AJR Am J Roentgenol. 194:1658–1663. [PubMed: 20489110]
18. Jansen SA, Shimauchi A, Zak L, et al. Kinetic curves of malignant lesions are not consistent across MRI systems: need for improved standardization of breast dynamic contrast-enhanced MRI acquisition. AJR Am J Roentgenol. 2009; 193:832–839. [PubMed: 19696299]
19. Esserman L, Hylton N, George T, Weidner N. Contrast-Enhanced Magnetic Resonance Imaging to Assess Tumor Histopathology and Angiogenesis in Breast Carcinoma. Breast J. 1999; 5:13–21. [PubMed: 11348250]
20. Holm S. A simple sequentially rejective multiple test procedure. Scand J Statist. 1979; 6:65–70.
21. Heywang-Kobrunner SH, Bick U, Bradley WG Jr, et al. International investigation of breast MRI: results of a multicentre study (11 sites) concerning diagnostic parameters for contrast-enhanced MRI based on 519 histopathologically correlated lesions. Eur Radiol. 2001; 11:531–546. [PubMed: 11354744]
22. Schnall MD, Blume J, Bluemke DA, et al. Diagnostic architectural and dynamic features at breast MR imaging: multicenter study. Radiology. 2006; 238:42–53. [PubMed: 16373758]
23. Bartella L, Thakur SB, Morris EA, et al. Enhancing nonmass lesions in the breast: evaluation with proton (1H) MR spectroscopy. Radiology. 2007; 245:80–87. [PubMed: 17885182]
24. Liberman L, Morris EA, Lee MJ, et al. Breast lesions detected on MR imaging: features and positive predictive value. AJR Am J Roentgenol. 2002; 179:171–178. [PubMed: 12076929]

25. Sakamoto N, Tozaki M, Higa K, et al. Categorization of non-mass-like breast lesions detected by MRI. Breast Cancer. 2008; 15:241–246. [PubMed: 18224381]
26. Tozaki M, Fukuda K. High-spatial-resolution MRI of non-masslike breast lesions: interpretation model based on BI-RADS MRI descriptors. AJR Am J Roentgenol. 2006; 187:330–337. [PubMed: 16861534]
27. Yabuuchi H, Matsuo Y, Kamitani T, et al. Non-mass-like enhancement on contrast-enhanced breast MR imaging: Lesion characterization using combination of dynamic contrast-enhanced and diffusion-weighted MR images. Eur J Radiol. 2009; 75:15–20.
28. Bartella L, Liberman L, Morris EA, Dershaw DD. Nonpalpable mammographically occult invasive breast cancers detected by MRI. AJR Am J Roentgenol. 2006; 186:865–870. [PubMed: 16498122]
29. Goto M, Ito H, Akazawa K, et al. Diagnosis of breast tumors by contrast-enhanced MR imaging: comparison between the diagnostic performance of dynamic enhancement patterns and morphologic features. J Magn Reson Imaging. 2007; 25:104–112. [PubMed: 17152054]
30. Liberman L, Morris EA, Dershaw DD, Abramson AF, Tan LK. Ductal enhancement on MR imaging of the breast. AJR Am J Roentgenol. 2003; 181:519–525. [PubMed: 12876038]
31. Rosen EL, Smith-Foley SA, DeMartini WB, Eby PR, Peacock S, Lehman CD. BI-RADS MRI enhancement characteristics of ductal carcinoma in situ. Breast J. 2007; 13:545–550. [PubMed: 17983393]
32. Li KL, Henry RG, Wilmes LJ, et al. Kinetic assessment of breast tumors using high spatial resolution signal enhancement ratio (SER) imaging. Magn Reson Med. 2007; 58:572–581. [PubMed: 17685424]
33. Li KL, Partridge SC, Joe BN, et al. Invasive breast cancer: predicting disease recurrence by using high-spatial-resolution signal enhancement ratio imaging. Radiology. 2008; 248:79–87. [PubMed: 18566170]
34. Chen W, Giger ML, Bick U, Newstead GM. Automatic identification and classification of characteristic kinetic curves of breast lesions on DCE-MRI. Med Phys. 2006; 33:2878–2887. [PubMed: 16964864]
35. Williams TC, DeMartini WB, Partridge SC, Peacock S, Lehman CD. Breast MR imaging: computer-aided evaluation program for discriminating benign from malignant lesions. Radiology. 2007; 244:94–103. [PubMed: 17507720]
36. Jansen SA, Fan X, Medved M, et al. Characterizing early contrast uptake of ductal carcinoma in situ with high temporal resolution dynamic contrast-enhanced MRI of the breast: a pilot study. Phys Med Biol. 2010; 55:N473–485. [PubMed: 20858914]
37. Sardanelli F, Rescinito G, Giordano GD, Calabrese M, Parodi RC. MR dynamic enhancement of breast lesions: high temporal resolution during the first-minute versus eight-minute study. J Comput Assist Tomogr. 2000; 24:724–731. [PubMed: 11045693]
38. Veltman J, Stoutjesdijk M, Mann R, et al. Contrast-enhanced magnetic resonance imaging of the breast: the value of pharmacokinetic parameters derived from fast dynamic imaging during initial enhancement in classifying lesions. Eur Radiol. 2008; 18:1123–1133. [PubMed: 18270714]
39. Harms SE. The use of breast magnetic resonance imaging in ductal carcinoma in situ. Breast J. 2005; 11:379–381. [PubMed: 16297079]
40. Kuhl CK, Braun M. Magnetic resonance imaging in preoperative staging for breast cancer: pros and contras. Radiologe. 2008; 48:358–366. [PubMed: 18369582]
41. Lehman CD, Isaacs C, Schnall MD, et al. Cancer yield of mammography, MR, and US in high-risk women: prospective multi-institution breast cancer screening study. Radiology. 2007; 244:381–388. [PubMed: 17641362]
42. Neubauer H, Li M, Kuehne-Heid R, Schneider A, Kaiser WA. High grade and non-high grade ductal carcinoma in situ on dynamic MR mammography: characteristic findings for signal increase and morphological pattern of enhancement. Br J Radiol. 2003; 76:3–12. [PubMed: 12595319]
43. Van Goethem M, Schelfout K, Kersschot E, et al. Comparison of MRI features of different grades of DCIS and invasive carcinoma of the breast. Jbr-Btr. 2005; 88:225–232. [PubMed: 16302331]
44. Jansen SA, Paunesku T, Fan X, et al. Ductal carcinoma in situ: X-ray fluorescence microscopy and dynamic contrast-enhanced MR imaging reveals gadolinium uptake within neoplastic mammary ducts in a murine model. Radiology. 2009; 253:399–406. [PubMed: 19864527]

45. Jansen SA, Fan X, Yang C, Shimauchi A, Karczmar G, Newstead GM. Relating dose of contrast media administered to uptake and washout of malignant lesions on DCEMRI of the breast. Acad Radiol. 2010; 17:24–30. [PubMed: 19836270]

46. Bhooshan, N.; Giger, ML.; Edwards, D., et al. Medical Imaging 2009: Computer Aided Diagnosis. Vol. 7260. SPIE; 2009. Using three-class BANN classifier in the automated analysis of breast cancer lesions in DCE-MRI; p. 72600J-72600J.

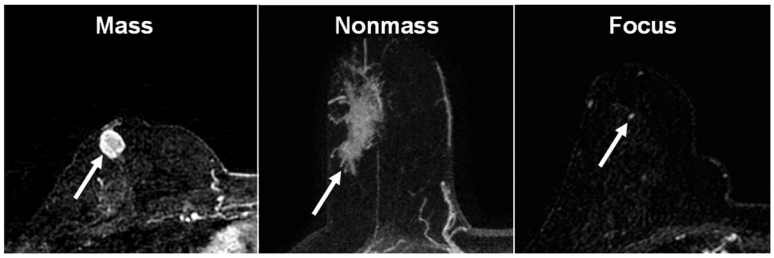

Fig. 1.

T_1 weighted axial post-contrast subtraction images demonstrating: a) mass-like enhancement in a 47 year old woman representing IDC, b) nonmass-like enhancement in a 54 year old woman representing DCIS, and c) focus enhancement in a 61 year old woman representing DCIS.

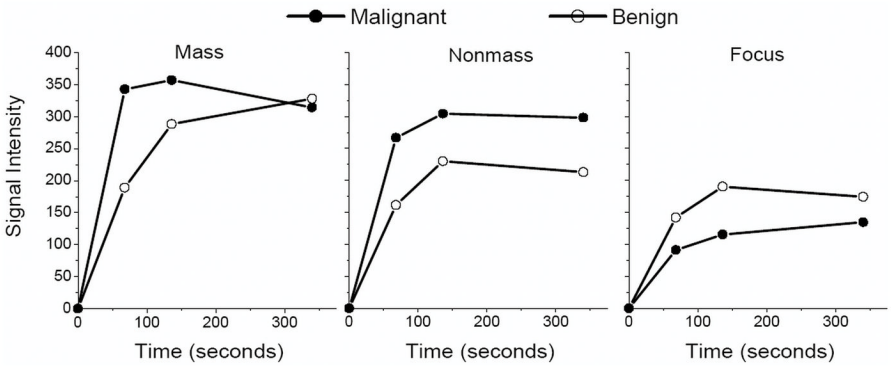

Fig. 2.

Representative kinetic curves of malignant and benign lesions of each enhancement type: a) mass-like enhancement: malignant IDC and benign fibrocystic change (FCC), b) nonmass-like enhancement: malignant DCIS and benign FCC, and c) focus enhancement: malignant DCIS and benign FCC.

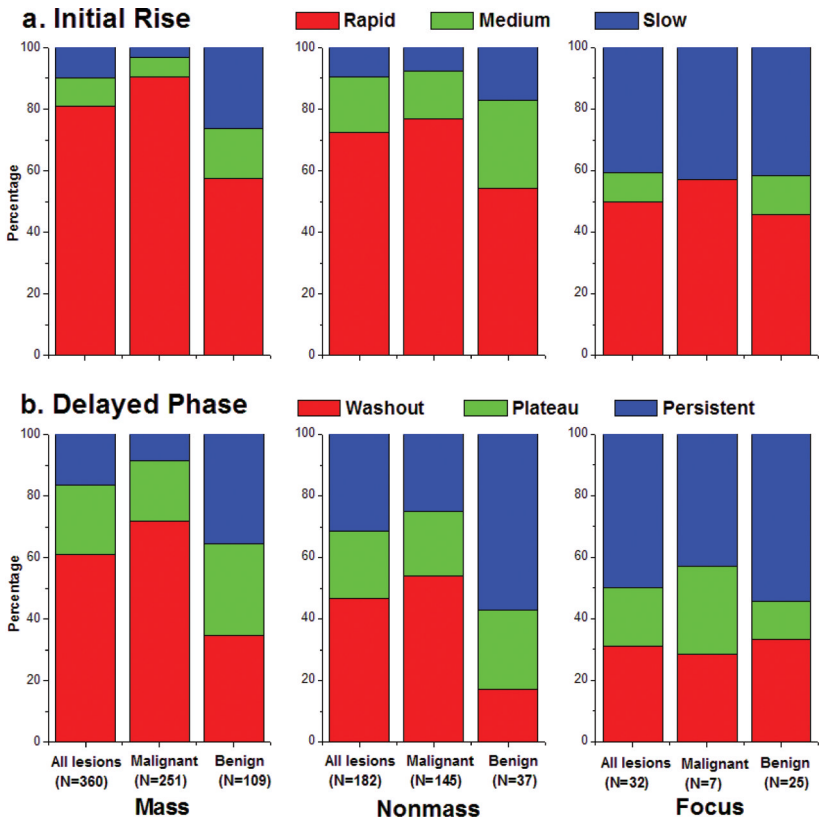

Fig. 3.

BIRADS qualitative descriptors of a) initial rise and b) delayed phase, in mass, nonmass and focus lesions overall, as well as benign and malignant subtypes.

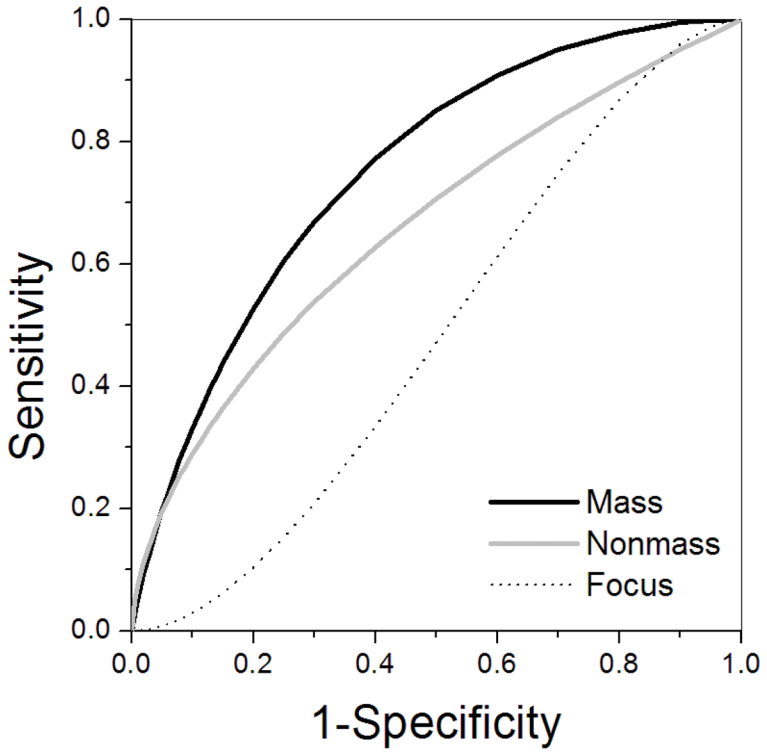

Fig. 4.
ROC curves of the parameter **SER** in focus lesions (dashed line), mass lesions (dark grey line), and nonmass lesions (light grey line). This plot demonstrates improved diagnostic performance of **SER** in mass compared with nonmass and focus lesions.

Table 1

Imaging systems and acquisition parameters used and total number of lesions.

	System A	System B	System C
Magnet	1.5T GE Genesis Signa	1.5T GE Signa Excite	1.5T Philips Achieva
Acquisition plane	Coronal	Axial	Axial
Pulse sequence	3D SPGR	3D FGRE	3D FFE
TR/TE (ms)	7.7/4.2	4.3/2.0	7.9/3.9
Flip angle (degree)	30	10	10
Slice thickness (mm)	3.00	2.00	2.00
In plane resolution (mm)	1.4	0.82	0.94
Temporal resolution (s)	68	58	55
# of post-contrast	3 or 5[a]	4 or 6	4 or 6 [b]
Fat suppression (y/n)	n	y	y
Parallel imaging (y/n)	n	y	y
Total benign lesions (#mass, #nonmass, #focus)	171 (109, 37, 25)	33 (22,7,4)	31 (25,5,1)
Total malignant lesions (#mass, #nonmass, #focus)	403 (251,145,7)	99 (69,28,2)	115 (76,39,0)

[a]The first two post-contrast images were acquired every 68 seconds. For the five point dynamic protocol, the remaining three images were acquired with 68 second resolution. For the three point dynamic protocol, the first two post-contrast acquisitions were followed by acquisition of high spatial resolution sagittal images for 128 seconds, and returning to a final dynamic, 68 second, acquisition.

[b]For Systems B and C, the first post-contrast acquisition was again started 20 seconds after contrast injection and the first three post-contrast images were acquired every 55–58 seconds. For the six point dynamic protocol, the remaining three images were acquired with 55–58 second resolution. For the four point dynamic protocol, the first two post-contrast acquisitions were followed by acquisition of high spatial resolution sagittal images and returning to a final dynamic acquisition.

Table 2

Pathology classification of focus, mass and nonmass lesions. The overall numbers and sizes of benign and malignant lesions are noted, as well as the pathological subtypes.

Type of lesions	Overall No. (n=852)	Size (mm)	Mass (n=552)	Nonmass (n=261)	Focus (n=39)
All Benign	**235**	**11.1±7.9**	**156**	**49**	**30**
Fibroadenoma	51	11.1±4.9	44	5	2
Papilloma	34	10.3±4.7	24	9	1
FCC	62	13.6±12.2	30	21	11
Breast tissue	46	8.7±4.7	32	4	10
Other	42	10.3±7.2	26	10	6
All Malignant	**617**	**25.6±20.3**	**396**	**212**	**9**
DCIS	136	25.3±22.0	28	103	5
IDC	373	25.3±19.1	299	71	3
ILC	41	20.7±12.7	23	18	0
Other	67	30.5±24.9	46	20	1

Table 3

Quantitative kinetic parameters of focus, mass and nonmass lesions stratified by pathology as benign or malignant. The *p* values of *t*-test comparisons of benign and malignant lesions within each type of enhancement pattern for each parameter are also shown.

Type of lesions	No. cases	E_1 (%)	E_{peak} (%)	T_{peak} (sec)	SER
All Mass	**360**	**285±156**	**348±161**	**167±102**	**1.02±0.49**
Malignant	251	310±155	354±157	144±91	1.13±049
Benign	109	219±143	333±171	228±105	0.76±0.36
p-value		$< 10^{-6}$	0.3	$< 10^{-9}$	$< 10^{-12}$
All Nonmass	**182**	**210±130**	**265±146**	**209±111**	**0.90±0.34**
Malignant	145	219±132	274±147	202±109	0.93±0.35
Benign	37	166±109	227±133	245±121	0.76±0.28
p-value		0.03	0.1	0.09	0.008
All Focus	**32**	**152±154**	**225±176**	**251±100**	**0.77±0.39**
Malignant	7	124±56	204±125	276±87	0.75±0.30
Benign	57	161±175	231±191	243±105	0.77±0.2
p-value		0.4	0.7	0.4	0.9

Table 4

Diagnostic performance of the quantitative kinetic parameters **E_1**, **E_{peak}**, **SER** and **T_{peak}**. Area under the curve (A_z) values, calculated from generated ROC curves, are displayed with 95% confidence intervals in parentheses.

	Overall	Mass	Nonmass	Focus
E_1 (%)	0.65 (0.59, 0.70)	0.66 (0.60, 0.73)	0.61 (0.49,0.72)	0.49 (0.27,0.70)
E_{peak} (%)	0.56 (0.50,0.62)	0.54 (0.47, 0.61)	0.60 (0.48,0.72)	0.47 (0.26, 0.68)
T_{peak} (sec)	0.67 (0.61,0.72)	0.72 (0.65, 0.78)	0.58 (0.44,0.70)	0.53 (0.25,0.79)
SER	0.71 (0.66,0.76)	0.75 (0.69,0.81)	0.670.55,0.76)	0.48(0.27,0.70)